Bulletin of JSME, Vol. 27, No. 233, November 1984

Paper No. 83—0106

Oscillatory Motion of Natural Convection in Rectangular Cavity*

By Kenzo KITAMURA**, Kimikazu KOMIYAMA***, and Takeshi SAITO****

An oscillatory motion of natural convection in a rectangular cavity has been studied both experimentally and analytically. Experiments were conducted mainly in the case that the hot and cold surfaces were set up as the upper and lower half walls of a side plate, and the other walls were insulated. A periodic oscillation of the hot and cold cells was found to occur by the flow visualization in a certain range of the Rayleigh numbers. The influences of the Prandtl number and the aspect ratios of the cavity on the oscillation frequency were also examined. Unsteady two-dimensional equations, which govern a laminar natural convection, were solved numerically to simulate the oscillation. The calculated flow patterns and oscillation frequencies were in fairly good agreement with the experiments. From these facts, the applicability of above numerical schemes to the other systems of the oscillations was discussed.

Key Words : Convective Heat Transfer, Natural Convection in Enclosure, Oscillatory Motion, Transition Phenomena, Flow Visualization, Unsteady Analysis

1. Introduction

An oscillatory motion of natural convection in an enclosed cavity has been observed by several investigators. Powe et al.(1) made a flow visualization of natural convection within horizontal concentric annuli and found that an ascending flow from the top of a heated inner cylinder began to oscillate at a certain critical Grashof number in the case of small gap width. Igarashi(2),(3) reported similar oscillations of the ascending flow from a line heat source which was stretched horizontally in a rectangular or cylindrical cavity as shown in Fig.1(a). These oscillations can be grouped as an oscillation of ascending flow.

Contrary to this, a different type of oscillation is presented in this paper. We tentatively call it oscillation of horizontal flow. This oscillatory motion occurs between unstably stratified hot and cold cells in a rectangular cavity. One of typical flow configurations and thermal boundary conditions are presented in Fig.1(b).

These oscillating flows have received increasing attention in recent years. This is due in part to recognition of the importance of natural convection at high Rayleigh numbers. In many applications such as passive solar house, thermal energy storage, and crystal growth, regularly or irregularly oscillating fluid motions caused by a natural convection often take place. Therefore, it is worth while to classify and make clear the fundamental mechanism of oscillations.

In the present paper, main concern is focused on the oscillation of horizontal flow in the case of Fig.1(b), in which only Küblbeck et al.(4) predicted its existence analytically. Their numerical scheme and obtained results, however, have contained some errors, and it was doubtful whether the actual phenomena could be simulated.

Considering the above, detailed experiments in the case of Fig.1(b) are conducted. The flow patterns within a rectangular cavity are categorized into three regimes; steady, periodically oscillating, and irregularly oscillating(turbulent) natural convection, respectively. Especially in the periodically oscillating regime, the onset and the end of oscillation and also the oscillation frequency are measured. The effects of Prandtl number and the aspect ratios of the cavity on the oscillation are examined experimentally.

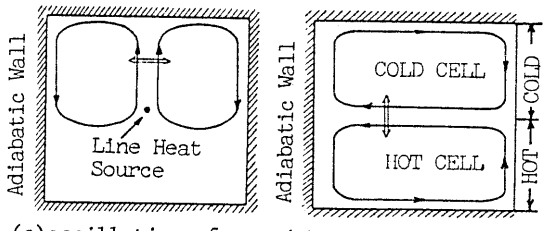

(a) oscillation of ascending flow

(b) oscillation of horizontal flow

Fig.1 Oscillatory flow

* Received 9th May, 1983

** Lecturer, *** Graduate Student,
**** Professor Emeritus, Department of Energy Engineering, Toyohashi University of Technology (1-1 Tempaku-cho, Toyohashi 440, Japan)

The momentum and energy transport equations, which govern an unsteady two-dimensional natural convection, are solved numerically to simulate the oscillation. It is revealed that the analytical results well predict the oscillatory flow and heat transfer. The three-dimensional behavior of convection in a cavity is also investigated experimentally.

Summarizing these results, general guidelines are proposed to show under what flow configurations and thermal boundary conditions the oscillation should appear. Several oscillatory motions of ascending and horizontal flows are newly found by using these guidelines. The applicability of above numerical schemes to these oscillatory flows is also discussed.

Nomenclature

a: overall height of the heat transfer surface(see Fig.2)
A: cross-sectional aspect ratio($=b/a$)
b: width of the cavity(see Fig.2)
c: length of the cavity(see Fig.2)
C: lateral aspect ratio($=c/a$)
f: oscillation frequency
f^+: dimensionless frequency of oscillation ($=fa^2/\nu$)
g: gravitational acceleration
h: heat transfer coefficient
Nu: Nusselt number($=ha/\lambda$)
Pr: Prandtl number($=\nu/\alpha$)
Ra: Rayleigh number($=g\beta(T_h-T_c)a^3/\alpha\nu$)
T : temperature
u,v: velocities in the x and y directions
u^*,v^*: dimensionless velocities ($=u/u_0$ or v/u_0)
u_0 : characteristic velocity($=\alpha/a$)
x: co-ordinate in the horizontal direction(see Fig.2)
x^*: dimensionless co-ordinate($=x/a$)
y: co-ordinate in the vertical direction(see Fig.2)
y^*: dimensionless co-ordinate($=y/a$)
z: co-ordinate in the lateral direction(see Fig.2)
α: thermal diffusivity
β: volumetric coefficient of expansion with temperature
ψ,ψ^*: stream function and dimensionless stream function($=\psi/\alpha u_0$)
λ: wavelength and thermal conductivity
ω,ω^*: vorticity and dimensionless vorticity ($=a\omega/u_0$)
ν: kinematic viscosity
θ: dimensionless temperature($=(T-T_c)/(T_h-T_c)$)
τ,τ^*: time and dimensionless time($=\tau\alpha/a^2$)

2. Experimental Apparatus and Measurements

The present experiment was conducted with a rectangular cavity as schematically illustrated in Fig.2. The heat transfer surface consisted of a pair of copper plates of the same size. The upper plate was cooled by the chilled water and the lower plate was heated by an electric current through the stainless foil heaters, which were embeded behind the copper plate and insulated electrically. Both plates were maintained at constant but different temperatures and installed on one side wall of the rectangular cavity.

Heat transfer surfaces of 20, 40, 60, and 80mm in overall height were utilized in the present experiments. The surface temperatures were monitored at several locations of the plates with Chromel-Alumel thermocouples of 100μm diameter, which were welded behind the copper plates. The temperature distribution shows an acceptable uniformity within the range of ±0.25K for each plate.

All the walls of the cavity were constructed with acrylic resin plates of 10mm thickness. In order to make a flow visualization and a temperature measurement within the cavity, the slit and the small holes were installed at the top or counter wall.

Air and partly water were used as a working fluid. The temperature difference between the hot and cold isothermal plates was kept within the range of 5 to 30K, and the bulk fluid temperature was maintained equal to the ambient room temperature. This was an arrangement to insulate the walls of the cavity except for the heat transfer surface.

A C-A thermocouple probe of 50μm diameter was used for the fluid temperature measurements. The flow visualization was achieved by a transverse illumination in the x-y plane, and tabacco smoke for air and aluminum powder for water were introduced into the cavity to render the flow pattern visible.

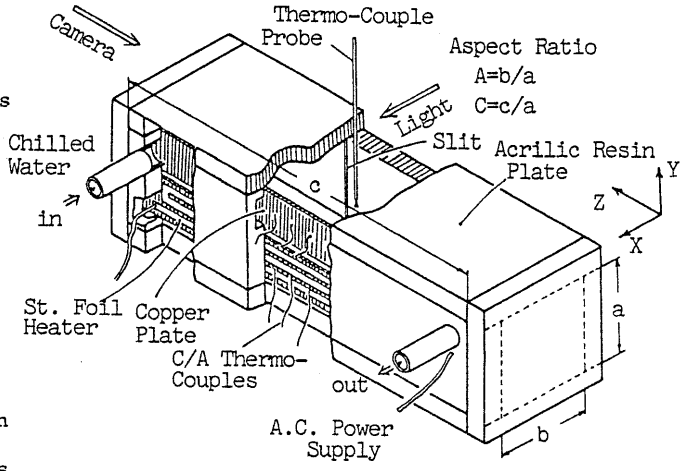

Fig. 2 Experimental apparatus

3. Numerical Analysis

The numerical analysis and calculation techniques for a laminar and two-dimensional natural convection in an enclosed cavity have been developed by many previous workers(4)-(6). Present analysis was done by almost the same procedures as above except for some corrections in the stability and convergence for the numerical calculations. Therefore, the following descriptions are limited to the outline of our analysis.

The following three conditions are assumed to simplify the problem:

1) The flow in the cavity is two-dimensional, laminar, and incompressible.
2) Physical properties of the fluid are constant except for a gravitational term.
3) Usual Boussinesq approximation can be applied.

Thus the governing equations for a nat-

ural convection in Cartesian co-ordinate systems are non-dimensionalized and represented as follows;
Energy transport equation:

$$\partial\theta/\partial\tau^* + u^*\partial\theta/\partial x^* + v^*\partial\theta/\partial y^* = \partial^2\theta/\partial x^{*2} + \partial^2\theta/\partial y^{*2} \quad \cdots\cdots(1)$$

Vorticity transport equation:

$$\partial\omega^*/\partial\tau^* + u^*\partial\omega^*/\partial x^* + v^*\partial\omega^*/\partial y^* = P_r(\partial^2\omega^*/\partial x^{*2} + \partial^2\omega^*/\partial y^{*2}) + G_rP_r^2\partial\theta/\partial x^* \quad \cdots\cdots(2)$$

Poisson equation for stream function:

$$\omega^* = -(\partial^2\psi^*/\partial x^{*2} + \partial^2\psi^*/\partial y^{*2}) \quad \cdots\cdots(3)$$

where the asterisks in the above equation indicate non-dimensionalized values as follows;

$$\left.\begin{aligned} &x^* = x/a,\ y^* = y/a,\ u^* = u/u_0 \\ &v^* = v/u_0,\ \omega^* = a\omega/u_0,\ \psi^* = \psi/(au_0) \\ &\tau^* = a\tau/a^2,\ P_r = \nu/a, \\ &\theta = (T - T_c)/(T_h - T_c) \\ &G_r = g\beta(T_h - T_c)a^3/\nu^2, \\ &u_0 = a/a,\ R_a = G_rP_r \end{aligned}\right\} \quad \cdots\cdots(4)$$

Following boundary conditions are given;

$$\left.\begin{aligned} &\theta_w = 1 \ (0 < y^* < 1/2) \\ &\theta_w = 0 \ (1/2 < y^* < 1) \end{aligned}\right\} \quad \text{at } x^* = b/a \quad \cdots\cdots(5)$$

$$\left.\begin{aligned} &(\partial\theta/\partial x^*)_w = 0 \quad \text{at } x^* = 0 \\ &(\partial\theta/\partial y^*)_w = 0 \quad \text{at } y^* = 0,\ 1 \end{aligned}\right\} \quad \cdots\cdots(6)$$

$$\left.\begin{aligned} &\psi_w^* = 0 \quad \text{at walls} \\ &\omega_w^* = -2\psi_{w-1}^*/\Delta x^{*2} \quad \text{at side walls} \\ &\omega_w^* = -2\psi_{w-1}^*/\Delta y^{*2} \quad \text{at top and bottom walls} \end{aligned}\right\} \quad \cdots(7)$$

Also the initial conditions are;

$$\left.\begin{aligned} &\theta = 1/2 \\ &\psi^* = \omega^* = u^* = v^* = 0 \end{aligned}\right\} \quad \text{at } \tau \le 0 \quad \cdots\cdots(8)$$

The spatial second order derivatives of the diffusion terms of Eqs.(1)-(3) and the convective terms of Eqs.(1) and (2) are approximated by using the second order central and upwind differences, respectively. The latter differentiation method is adopted to achieve stable numerical calculations.

The finite difference equations of Eqs. (1) and (2) are solved by using the ADI method because relatively large time steps are permitted. Eq.(3) is calculated by the SOR method for each time step until iterated values become less than a certain limit.

4. Results and Discussions

4.1. Visualization of oscillatory flow and numerical result

In order to categorize the flow patterns in a rectangular cavity as shown in Fig. 1(b), visualization is made to take instantaneous photos for comparison with the analytical result computed with the same *Ra* and *Pr* numbers. The following several sets of photos correspond to the experimental conditions of a cross-sectional aspect ratio *A=1* (square cavity) and a lateral aspect ratio *C=5*. Figs.3 and 4 represent the stream lines in the low *Ra* number region and they are both obtained from the experiments and analysis, respectively.

The analytical results in Fig.4 are plotted as contour bands, each representing 10% of the overall difference between maximum and minimum values of a stream function. The same illustration is made about the isothermal bands as presented in Fig.7(b). In Fig.3, the low temperature cell at the upper and the high temperature cell at the lower part in the cavity rotated steadily in the clockwise and counter-clockwise directions, respectively. The working fluid is air. These steadily rotating cells were also confirmed by the analysis as shown in Fig.4.

With a gradual increase in *Ra* number, the interface between hot and cold cells begins to fluctuate and finally an oscillation with reciprocal enlargement and recession of each cell occurs. These oscillatory flow patterns for air are photographed continuously at a constant time interval through one period of the oscillation and presented in Fig.5.

The same phenomena are observed with water. The visualized and computed results with the stream lines and the temperature distributions are compared under the same conditions and shown in Fig.6, Fig.7(a), and (b), respectively. From the stream lines presented in Figs.6 and 7(a), it is seen that the present analysis well predicts the

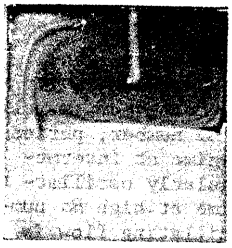

Fig.3 Steady rotating cells at low *Ra* No.(*Ra* $=7.03\times10^4$, *a=40mm, air*)

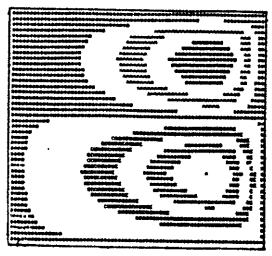

Fig.4 Analytical result of stream function in the case of Fig.3

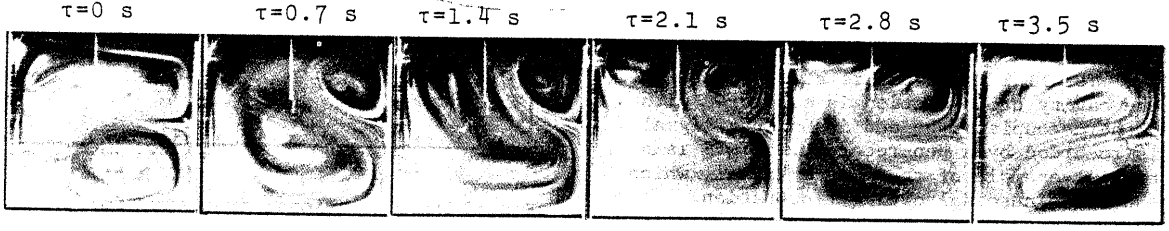

Fig.5 Visualization of periodically oscillating flow($Ra=2.06\times10^5$, *a=40mm, air*)

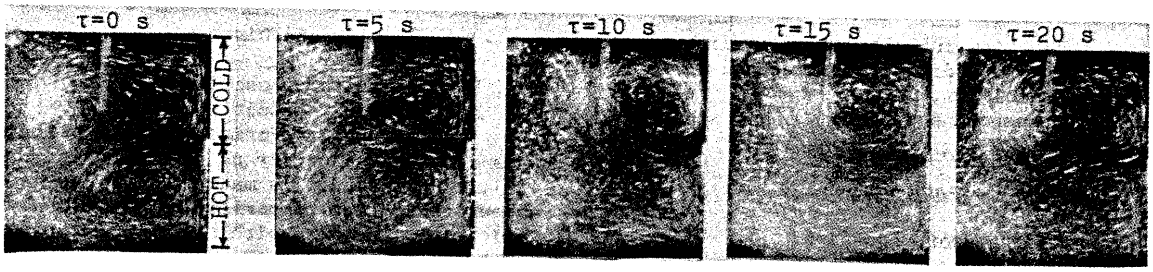

Fig.6 Visualization of periodically oscillating flow($Ra=7.23\times10^5$, $a=20mm$, water)

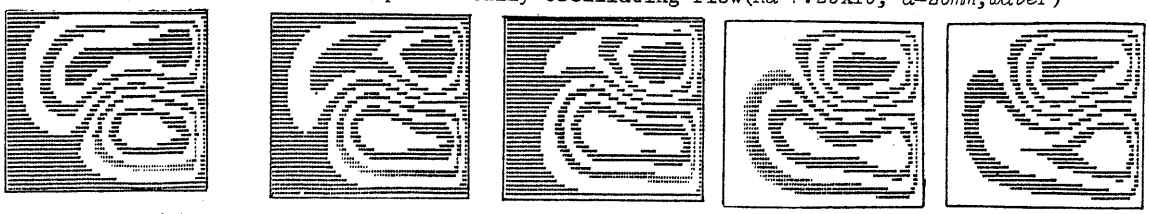

Fig.7(a) Analytical result of stream function in the case of Fig.6

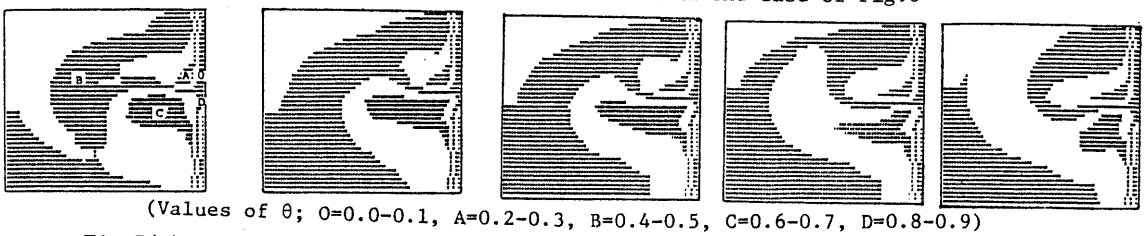

(Values of θ; O=0.0-0.1, A=0.2-0.3, B=0.4-0.5, C=0.6-0.7, D=0.8-0.9)

Fig.7(b) Analytical result of temperature distribution in the case of Fig.6

actual phenomena in its flow patterns and oscillation period, though there are some differences in the locations of cell centers. The calculated temperature distributions also indicate that the high and low temperature regions penetrate into each other with the enlargement and recession of cells.

With further increase in *Ra* number, there appear small cells at the corners of the cavity. The flow patterns in the cavity show complicated three-dimensional features and the oscillating flow gradually loses its periodicity. But even at the maximum *Ra* number, $Ra\simeq6\times10^6$, which we can attain, the oscillation of hot and cold cells is still observed as is presented in Fig.8. The computed results at the same *Ra* number show the oscillation at first several time steps, but diverge finally.

Summarizing these results, the flow patterns in the present rectangular cavity can be classified into three regimes, namely, steady flow regime at low *Ra* number, periodically oscillating flow regime at intermediate *Ra* number, and irregularly oscillating or turbulent flow regime at high *Ra* number. The periodically oscillating flow is considered a laminar flow from the fact that the laminar analysis can simulate the oscillation. In the next section, special attention is paid to this periodically oscillating flow and the fundamental mechanisms of oscillation are investigated experimentally.

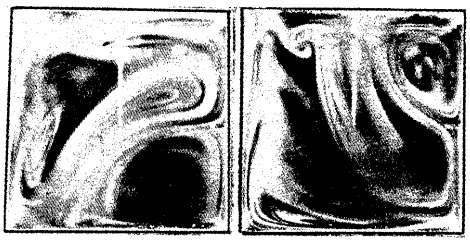

Fig.8 Irregularly oscillating cells at high *Ra* No.($Ra=1.08\times10^6$, $a=80mm$, air)

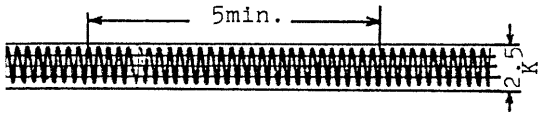

Fig.9 Output signals of temperature fluctuation($Ra=1.08\times10^6$, $a=80mm$, air)

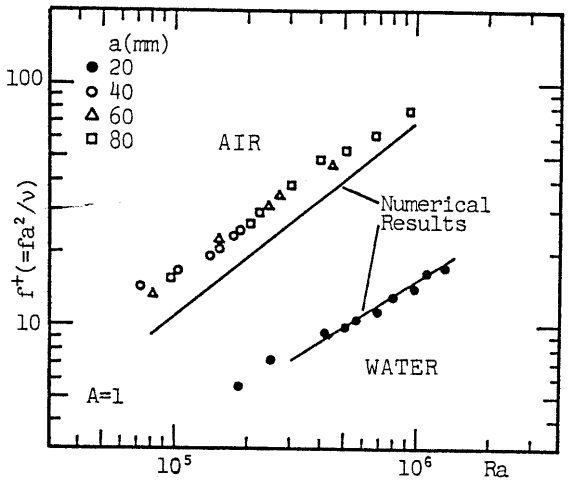

Fig.10 Non-dimensional frequency for periodically oscillating flow

4.2. Oscillation frequency and cavity flow

The fluid temperature at the center of the cavity cross-section is monitored with a thermocouple probe and its output signal is recorded by a pen-recorder. Fig.9 is a typical example of the output signal, which shows a sinusoidal cyclic fluctuation. The period of these temperature fluctuations is confirmed from a visualization to coin-

cide with the oscillation period of the flow in the cavity. Using this fact, the oscillation frequency is measured by counting the number of cycles per unit time.

The frequencies thus obtained are from *5* to *20 cycles/min.* for air and from *2* to *4 cycles/min.* for water in the present experiment. These frequencies are non-dimensionalized using a height of heat transfer surface and a kinematic viscosity of fluid and they are plotted with the *Ra* number as an abscissa. Fig.10 represents the results about the case of a square cavity. The numerical results are also illustrated for comparison. The start and end of the lines correspond with the computed onset and end of a periodic oscillation, respectively.

Non-dimensional frequencies are the linear functions of *Ra* number for each fluid of water and air. Comparing the frequencies obtained from the analysis with the experiment, they are in fairly good agreement in the case of water, and for air the former gives *10* to *20%* lower values than the latter, but their dependency on *Ra* number is quite similar. Also the onset and end of the oscillation are well predicted by the present analysis except for the onset of water.

The influence of aspect ratios of the cavity on the oscillation frequency is also examined experimentally by varying the cross-sectional aspect ratio *A* from *1/2* to *2* and the lateral aspect ratio *C* from *1* to *5*. It is revealed that the oscillation frequencies are little affected by the aspect ratios within the range of present work. But the onset and end of oscillation shift to the higher *Ra* numbers with a decrease of aspect ratio.

In order to answer the question whether the oscillation in the cavity can occur in the same phase throughout the lateral direction *z*, the flow patterns are visualized transversely at two cross-sections with different *z* locations. The experiments are conducted by using a pair of slits installed at the counter sidewall of the cavity. One of the representative photos is shown in Fig.11. As is obvious from the figure, the cold cell at near side is recessed to the corner and expanded at far side. This indicates that the phase of the oscillation differs in the *z* direction, and the flow in the cavity has a waviness.

Fig.11 Visualization of cavity flow at two cross-sections ($Ra=2.65\times10^5$, $a=40mm$, *air*)

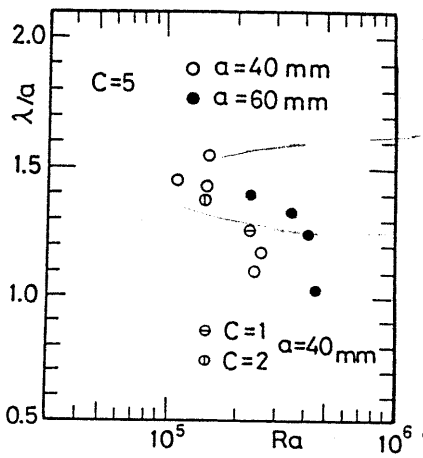

Fig.13 Wavelength in the *z*-direction

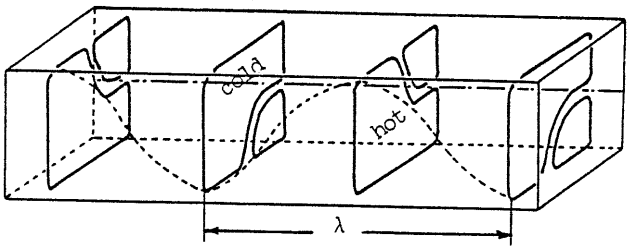

Fig.12 Schematical illustration of cavity flow

Summarizing these results, the flow patterns in the cavity are schematically illustrated in Fig.12. The magnitude of these waves is measured in the following way. A pair of thermocouple probes are located at the center of the cross-section. Their signals are monitored by a pen-recorder as shown in Fig.9. One of the two probes is fixed and the other is traversed in the *z*-direction, then the phase of recorded sinusoidal signals is shifted from each other with an increase of the distance between the two. At a certain distance in the *z*-direction, both signals oscillate in the same phase again. This distance is considered a wavelength of the oscillation and it is therefore measured under several conditions.

The wavelength thus obtained is normalized with a height of the heat transfer surface and plotted in Fig.13. *Ra* number is chosen as an abscissa. The wavelength of the oscillation is about *1* to *1.5* times greater than the height of the cavity and it becomes smaller with an increase of *Ra* number. The reason why this wavy feature can exist in the cavity has not been obvious. So the future work will be needed. However, from the fact that the oscillatory motion can be simulated by the two-dimensional analysis, the three-dimensional waves may not strongly affect the oscillation.

4.3. Heat transfer and oscillating flow

Time-averaged, overall heat transfer coefficients for the hot and cold surfaces are investigated to determine the influence of oscillation. The heat transfer coefficient for natural convection in a cavity is generally small. Especially as for the present case, the hot and cold surfaces are installed at the nearest location, and most of the heat deposited in the heater leaks out to the chilled water through the acrylic resin plate. Therefore, the surface heat flux, which is necessary to calculate the heat transfer coefficient, is measured using the heat flux extrapolated from the fluid temperature gradient near the heat transfer surface in this experiment.

Fig.14 represents the Nusselt number based on the time-averaged heat flux at the center of the heated plate. For comparison, the overall *Nu* number computed from the present analysis is also illustrated in the figure. The analytical result is time-averaged through one cycle of oscillation. Both data are obtained in the case of a square cavity. The *Nu* number is almost constant in the low *Ra* number region, and it increases abruptly beyond the critical *Ra* number. This *Ra* number corresponds to the onset of oscillation, in the present case the oscillation starts at $Ra\simeq8\times10^4$. Above result

indicates that the oscillatory flow in the cavity enhances the heat transfer very much, which is also confirmed by the present analysis.

4.4. Oscillation of horizontal and ascending flow

In the previous sections, main concerns were focused on the oscillation of horizontal flow, especially in the case of Fig.1(b). In this section, several discussions are made to answer the question under what flow field configurations and thermal boundary conditions the oscillatory flow could occur. The appearance of an oscillating flow has been believed to be a special case by the previous workers as was mentioned in Chapter 1. Reviewing these previous and present studies, the following conditions for the occurrence of the oscillations could be proposed:

(1) More than a pair of cells should exist in the cavity.

This is a premise, and

(2) In the case of an oscillation of ascending flow, the cell interface should be separated vertically,

or

(3) In the case of an oscillation of horizontal flow, the cell interface should be separated horizontally and should be thermally unstable.

These are necessary, though not sufficient, conditions for the occurrence of oscillations. Based on these guidelines (1) to (3), the thermal boundary conditions, which are illustrated in Figs.15(a) and (b), are selected and investigated to certify the oscillations of horizontal and ascending flow, respectively.

Fig.16 represents the visualized flow patterns for the boundary conditions of Fig. 15(a). The computed stream function distributions obtained with the same *Ra* and *Pr* numbers are also shown in Fig.17. The oscillation of horizontal flow, in which two pairs of hot and cold cells at the corners are recessed and elongated in the diagonal direction, is observed. It is obvious from Fig.17 that the present analysis succeeded in predicting the oscillation of horizontal flow.

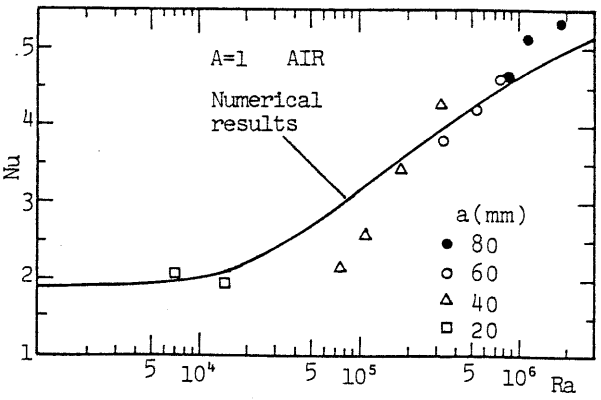

Fig.14 Oscillating flow and heat transfer coefficient

For the case of Fig.15(b), the oscillation of ascending flow is found to exist by the experiment. Photographs are presented in Fig.18 for a half period of the oscillation. On the other hand, the computed stream function distributions in Fig.19 show a steadily rotating pair of cells even at the same or much higher *Ra* number than the experiment.

The present analysis was also conducted to simulate the oscillation of ascending flow from the line heat source as was observed by Igarashi[3] but it failed.

From these results, two conclusions could be drawn. First, the occurrence of oscillatory flow in the cavity is not so special as has been considered, and can be forecast by using the above guidelines (1) to (3). Second, present numerical analysis simulates the oscillations of horizontal flow in its flow pattern and oscillation frequency, but is incapable of predicting the oscillation of ascending flow.

The oscillations of horizontal and ascending flow discussed above could be closely correlated with the stability problems of the thermally stratified flow and thermal plume, respectively. In view of the applicability of the present analysis, the fundamental mechanisms of both oscillations are thought to be quite different.

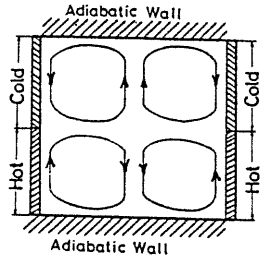

Fig.15(a) Oscillation of horizontal flow

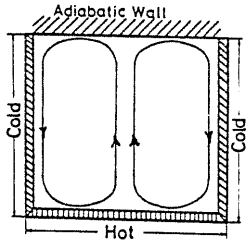

(b) Oscillation of ascending flow

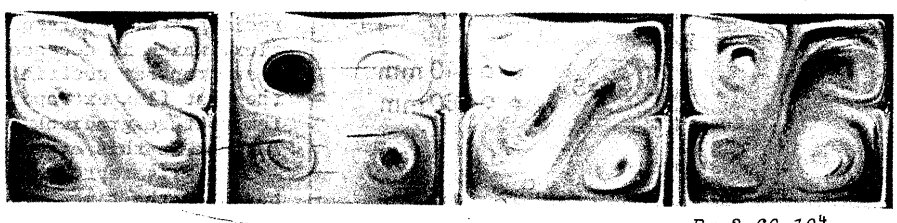

Fig.16 Oscillating flow in the case of Fig.15(a) ($Ra=2.60\times10^4$, $a=40mm$, air)

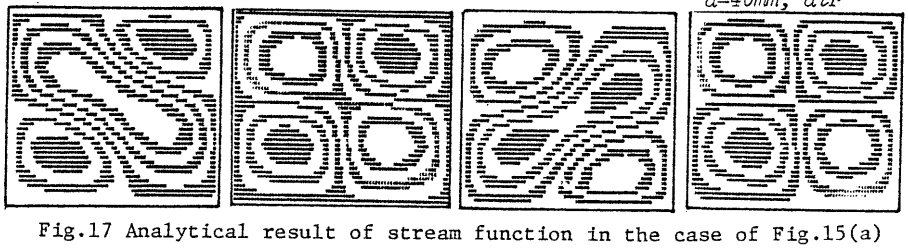

Fig.17 Analytical result of stream function in the case of Fig.15(a)

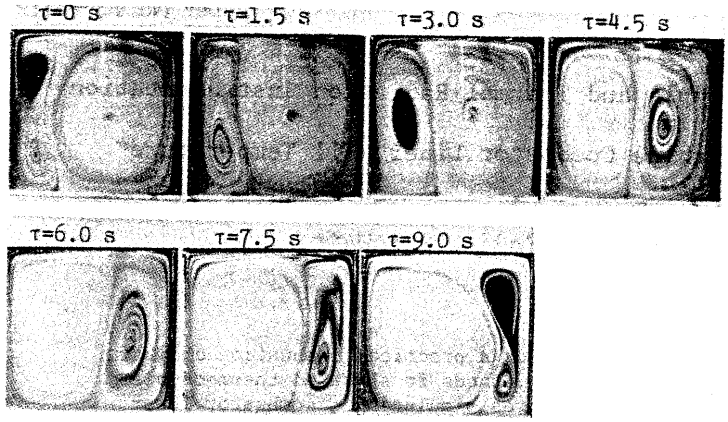

Fig.18 Visualization of oscillatory flow in the case of Fig.15(b) ($Ra=8.50\times10^4$, $a=40mm$, air)

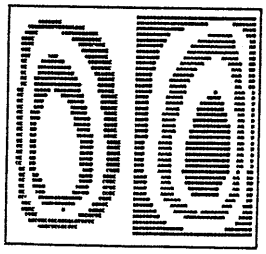

Fig.19 Analytical result of stream function in the case of Fig.15(b)

5. Concluding Remarks

The oscillatory motion of natural convection in a rectangular cavity, in which the hot and cold surfaces were mounted at the upper and lower half walls of a side plate, was mainly investigated in the present study.

Both the experiments and the analysis were conducted, and the following conclusions were obtained;

(1) The flow patterns in the cavity are classified into three regimes; steady, periodically oscillating, and irregularly oscillating or turbulent regimes, with an increase of Ra number.
(2) Present two-dimensional laminar flow analysis well predicts the steady and periodically oscillating flows.
(3) The non-dimensionalized frequency of the oscillation is determined by Ra number for each fluid of air and water.
and
(4) The heat transfers at the hot and cold surfaces are enhanced by the oscillatory flow.

The oscillating flows were newly found for several cases of natural convection in a rectangular cavity through the present experiments. It has been revealed that the present analysis can be applied to the horizontal flow oscillation.

Acknowledgement

Authors wish to acknowledge the financial support from the Ministry of Education, Science and Culture, Japan, through a research grant(No.57750163). They are also much indebted to Professor C.L.Tien (Univ. of California, Berkeley), who was formerly an invited professor of their university on a research fellowship sponsored by Japan Society for Promotion of Science, for numerous advices and instructive discussions throughout this study.

References

(1) Powe,R.R., Carley,C.T., and Bishop,E.H., Trans. Amer. Soc. Mech. Engrs., J. Heat Transfer, Vol.93, No.3 (1969-8), p.310.
(2) Igarashi,T., and Kada,M., Trans. Japan Soc. Mech. Engrs.(in Japanese), Vol.41, No.345 (1975-5), p.1500.
(3) Igarashi,T., Trans. Japan Soc. Mech. Engrs.(in Japanese), Vol.43, No.374 (1977-10), p.3839.
(4) Küblbeck,K., et al., Int. J. Heat Mass Transfer., Vol.23, No.2 (1980-2), p.203.
(5) Wilkes, J.O. and Churchill,S.W., Amer. Inst. Chem. Engrs., Vol.12, No.1 (1966-1), p.161.
(6) Cormack,D.E., Leal,L.G., and Imberger,J., J. Fluid Mech., Vol.65, No.1 (1974-1), p.231.